## ROBUST ADAPTIVE NEURAL TRACKING CONTROL FOR UNDERACTUATED NONLINEAR SYSTEMS: A ROTARY INVERTED PENDULUM CASE STUDY

NGUYEN HOANG HIEU, MAI THANG LONG, NGUYEN NGOC SON\*

Faculty of Electronics Technology, Industrial University of Ho Chi Minh City

\* Corresponding author: nguyenngocson@iuh.edu.vn

DOIs: https://www.doi.org/10.46242/jstiuh.v77i5.5610

**Abstract.** The underactuated system demonstrates significant coupling and highly nonlinear dynamics, posing challenges for precise control. This paper introduces an adaptive control approach for the underactuated rotary inverted pendulum (RIP) system. The objective is to enable the manipulator arm to track a desired trajectory and to maintain the pendulum in an upright position concurrently. The proposed method employs two neural networks: the first focuses on tracking the desired trajectory of the manipulator arm, while the second stabilizes the pendulum in its upright position. Stabilize the system using Lyapunov theory. To validate the effectiveness of the proposed control strategy, experiments are conducted using the NI-PCI 6221 data acquisition card with the RIP system. Both simulation and experimental results underscore the robustness of the proposed control method against system uncertainties and external disturbances, achieving stable operational performance.

Keywords. Adaptive neural control, underactuated system, rotary inverted pendulum

## 1 INTRODUCTION

An underactuated mechanical system (UMS) is a system that has more degrees of freedom (DOF) to be controlled than the number of independently controlled actuators exerting force or torque onto the system. A UMS offers many advantages including increased operational capacity (e.g., more degrees of freedom) without the need for additional hardware, and energy efficiency that are very attractive for unmanned aerial and underwater vehicles with limited resources and energy storage. Specifically, a UMS can offer a system design that costs and weighs significantly less without losing or reducing the configuration space. Although the modeling, formulation and control theory of UMS have been studied to a great extent in the last decade, the control of a UMS in practical applications including aerial and underwater vehicles remains a nontrivial task. Very interesting reviews and books have been published on this topic to emphasize the importance and applications of the UMS [1], [2], [3]. The condition of underactuation in mechanics, robotics, mechatronics, or dynamical systems refers to a system with more degrees of freedom (number of independent variables that define the system configuration) than actuators (input variables) to be controlled. This restriction implies that some of the configuration variables of the system cannot be directly commanded, which highly complicates the design of control algorithms.

The problem of finding an effective control law for an underactuated nonlinear system with fewer actuators than the number of degrees of freedom to control has attracted increasing attention because of its special properties. Systems with fewer actuators than degrees of freedom appear more and more in applications [4], such as underactuated UAVs [5], underactuated flexible joint robots [6], wheeled-bipedal robots [7], and underactuated AUVs [8]. In the presence of an actuator-free joint and a non-actuated free joint, it is not possible for conventional control to control the desired outputs well. Therefore, this system cannot follow the set signal arbitrarily.

To solve the problem, the classical linear control approaches are designed. For example, S.E. Oltean [9] proposed fuzzy-PD controllers for swing-up control and stability for the rotary inverted pendulum (RIP). Yang et al. [10] introduced a hybrid pole-placement controller and proportional—integral—derivative (PID) or fractional-order PID (FOPID) to simultaneously track the control and stabilization of the RIP system. Mathew et al. [11] developed the linear quadratic regulator (LQR) control for the RIP system. Nguyen et al. [12] proposed a hybrid control between the feedback linearization-based energy control methods. However, the above controllers have weaknesses such as the exact physical parameters are not known, or the mathematical model is not accurate, leading to the design of the controller being extremely difficult. Moreover, the control quality will not be good in different operating conditions and the stability of the system cannot be guaranteed in the presence of system uncertainties and disturbances.

To overcome the drawbacks of classical control, a hybrid linear control with modern control techniques such as sliding mode control (SMC), and fuzzy logic control (FLC) are considered. Hazem et al. [13] proposed a fuzzy-based LQR for stability control of a double-link RIP system. Bekkar et al. [14] proposed an online tuning LQR based on FLC for balancing and tracking control of the RIP system. In which, FLC was used to adjust the weighting matrices Q and R of LQR. However, the stability of FLC is difficult to confirm based on Lyapunov law. Therefore, Nguyen et al. [15] proposed a hybrid fuzzy-LQR and SMC for the swing-up and balancing control of the Pendubot system. In which, the SMC scheme was used for swing up and fuzzy-based LQR was applied for tracking and balancing control. Nagarajan et al. [16] proposed a hybrid PID and SMC control for the RIP system, in which the PID and SMC parameters were optimized by an improved whale optimization algorithm (WOA). Chawla et al. [17] introduced a combination of LQR and SMC for the robust control of the RIP system, where LQR for optimal performance and SMC for robust control. The strength of approaches is based on SMC and FLC which are designed based on the system dynamics without linearization and the stability of the system can be guaranteed. However, the control parameters of these approaches are not adaptive or self-adaptive in different operating condition or external disturbacnes. Furthermore, due to the sliding control characteristic, there is chattering phenomenon affecting the hardware of RIP system.

Recently, self-learning and adaptive control have received a lot of research attention. For example, Yang et al. [18] designed a swing-up strategy by using trajectory planning and the inertia effect. The hybrid adaptive neural network and linear matrix inequation control were designed for balancing and stabilization. Bhourji et al. [19] proposed reinforcement learning (RL) control based on proximal deterministic policy gradient to control the RIP system. Dao et al. [20] proposed an adaptive integral sliding-mode control using a reinforcement learning-based adaptive dynamic programming (ADP) strategy for the pendulum system to improve the tracking control quality. Sousy et al. [21] proposed an adaptive super-twisting PID-SMC controller for the stabilization of the RIP system. In which, a super-twisting PID-SMC component was used for stability control and an adaptive control was used to approximate the uncertain bounds of disturbances. Junior et al. [22] designed the model reference control-based recurrent paraconsistent neural network (RPNN) for tracking the trajectory of RIP system. Nghi et al. [23] proposed a combined LQR and online radial basis function neural network (NN) for stabilizing of RIP system. In which, RBFNN was used to cancel the systematic deviation and external disturbances. Saleem et al. [24] designed a stable online gainadjustment mechanism via state-error-dependent nonlinear-scaling functions to self-tun the coefficients of LQR. Hazem et al. [25] introduced novel LQR gains tuned by using radial basis neuro-fuzzy architecture for RIP system. Zeghlache et al. [26] developed an adaptive fuzzy fast terminal sliding mode control for the pendulum system. In which, fast terminal sliding mode control was designed to guarantee faults, uncertainties compensation, and chattering phenomenon reduction. The common point of these studies is to propose a classical SMC scheme to ensure stability and use NN/FLC model for adaptive control to cope with the system uncertainties.

In this paper, an adaptive control is proposed to control RIP system. In which, the first neural network focuses on tracking a desired trajectory for the manipulator arm, while the second one stabilizes the pendulum at its upright position.

The main contributions of this study are as follows,

- (1) The proposed control method is a combination of linear feedback and neural network adaptation, although not a new control method for MIMO nonlinear system, but the approach for the underactuated nonlinear systems is to propose a tracking error filter function that is different from the previous indirect adaptive control methods for full-order systems and adaptive sliding control. Thanks to the tracking error filter function proposed here, the matrix calculation with a non-square matrix due to lack of order is avoided, which is difficult to calculate (must go through the calculation of the pseudo-inverse matrix). This control method also avoids the oscillation of the control signal, the chattering phenomenon of the sliding control method.
- (2) Lyapunov stability analysis derives update laws for the two neural networks, enabling simultaneous stabilization of arm orientation and pendulum position
- (3) Simulation and experimental results are tested to prove the effectiveness of the proposed controller.

The rest of the paper is as follows. Section 2 shows the system dynamics and problem formulation. Section 3 designs the proposed controller and stability analysis. Section 4 presents the simulation results and discussion. Section 4 also presents an experimental configuration to test the effectiveness of the proposed approach. Finally, the conclusions are summarised in section 5.

## 2 SYSTEM DYNAMICS AND FORMULATION

## 2.1 System dynamic

The diagram and coordinates of the RIP system are described in Fig.1. The parameter notations of RIP system are described in Table 1.

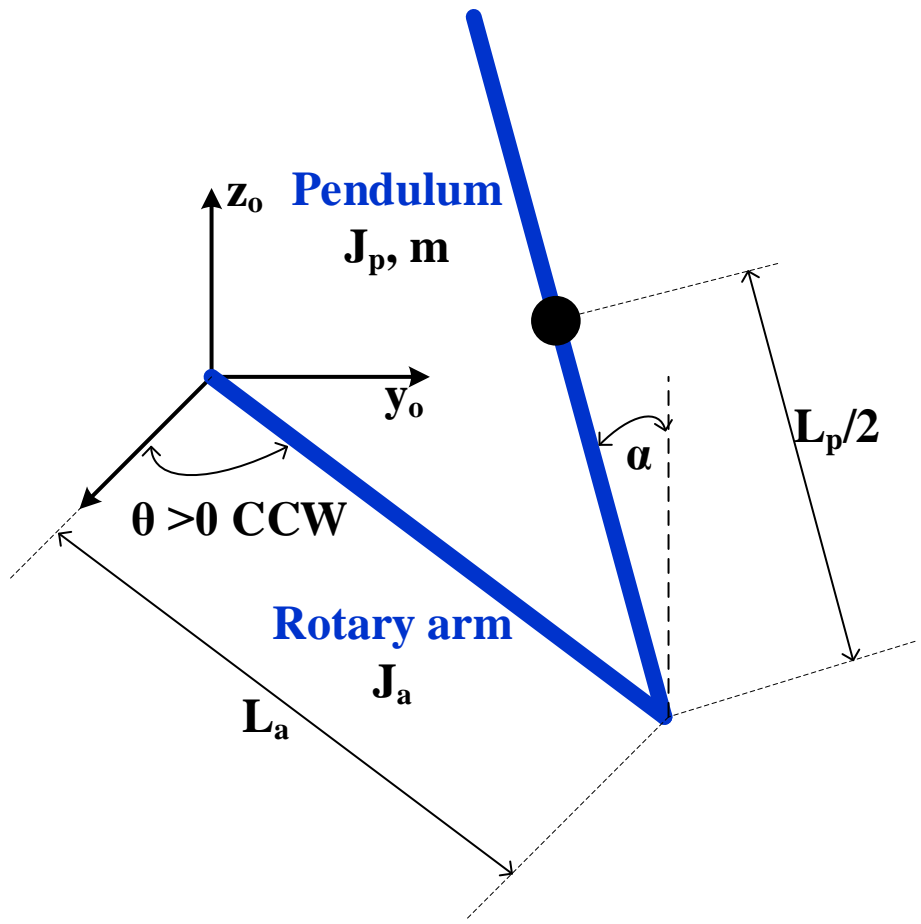


Fig.1. Schematic diagram of the RIP system

Table 1. Parameter notations of RIP system

No.	Parameters
$J_a$	Inertia of the arm
La	Total length of the arm
m	Mass of the pendulum
$L_p/2$	Distance to the center of gravity of the pendulum
$J_p$	Inertia of the pendulum around its center of gravity
$q_1$	Rotational angle of the arm
$q_2$	Rotational angle of the pendulum
u	Input torque applied on the arm

The dynamic model of the Rotary inverted pendulum can be written as,

$$M(q). \ddot{q} + V(q, \dot{q}). \dot{q} + G(q) = \tau \tag{1}$$

$$\begin{split} q &= \begin{bmatrix} q_1 \\ q_2 \end{bmatrix} = \begin{bmatrix} \theta \\ \alpha \end{bmatrix}; M(q) = \begin{bmatrix} P_1 + P_2 sin^2 \alpha & P_3 cos \alpha \\ P_3 cos \alpha & P_4 \end{bmatrix} \\ V(q, \dot{q}) &= \begin{bmatrix} \frac{1}{2} P_2 \dot{q}_2 \sin(2q_2) & -P_4 \dot{q}_2 sin(q_2) + \frac{1}{2} P_2 \dot{q}_1 \sin(2q_2) \\ -\frac{1}{2} P_2 \dot{q}_1 \sin(2q_2) & 0 \end{bmatrix} \\ G(q) &= \begin{bmatrix} 0 \\ -P_5 sin \alpha \end{bmatrix}; \ f_v(\dot{q}) = \begin{bmatrix} P_6 \dot{q}_1 \\ P_7 \dot{q}_2 \end{bmatrix}; \ \tau = \begin{bmatrix} u \\ 0 \end{bmatrix} \\ P_1 &= J_a + ml_a^2; \ P_2 = ml_p^2; \ P_3 = ml_a l_p; \ P_4 = J_p + ml_p^2; \ P_5 = mgl_p; P_6 = b_a; \ P_7 = b_p \end{bmatrix} \end{split}$$

## 2.2 Problem Formulation

Kinetic equations of state are as follows,

$$\dot{q}_1 = q_3 \tag{2}$$

$$\dot{q}_2 = q_4 \tag{3}$$

$$\dot{q}_3 = f_1 + g_1 u \tag{4}$$

$$\dot{q}_4 = f_2 + g_2 u \tag{5}$$

We denotes as,

$$f_1 = \frac{1}{\det(M)} [M_{22}H_1 - M_{12}.H_2] \tag{6}$$

$$f_2 = \frac{1}{\det(M)} [M_{11}H_2 - M_{21}.H_1] \tag{7}$$

$$H_1 = -C_{11}\dot{q}_1 - C_{12}\dot{q}_2 - P_6\dot{q}_1 \tag{8}$$

$$H_2 = -C_{21}\dot{q}_1 - C_{22}\dot{q}_2 - P_7\dot{q}_2 - P_5\sin(q_2) \tag{9}$$

$$H_{1} = -C_{11}\dot{q}_{1} - C_{12}\dot{q}_{2} - P_{6}\dot{q}_{1}$$

$$H_{2} = -C_{21}\dot{q}_{1} - C_{22}\dot{q}_{2} - P_{7}\dot{q}_{2} - P_{5}\sin(q_{2})$$

$$g_{1} = \frac{M_{22}}{\det(M)}, g_{2} = \frac{-M_{21}}{\det(M)}$$

$$(10)$$

Here, it is important to define a proper function of the error to gain the control goal as,
$$e = \begin{bmatrix} e_1 \\ e_2 \end{bmatrix} = \begin{bmatrix} q_{d1} - q_1 \\ q_{d2} - q_2 \end{bmatrix} = \begin{bmatrix} q_{d1} - q_1 \\ - q_2 \end{bmatrix} \in \mathcal{R}^2$$
(11)

Taking the derivative of Eq.11, we have,

$$\dot{e}_1 = \dot{q}_{d1} - \dot{q}_1 \tag{12}$$

$$\dot{e}_2 = -\dot{q}_2 \tag{13}$$

$$\ddot{e}_1 = \ddot{q}_{d1} - f_1 - g_1 u \tag{14}$$

**Assumption 1**. The desired trajectory of the arm of RIP system is that the signal  $q_{d1}$  is a smooth, seconddifferentiable, and bounded function.

$$||q_{d1}(t)||, ||\dot{q}_{d1}(t)||, ||\ddot{q}_{d1}(t)|| \le \delta \tag{16}$$

In which, delta is a positive constant.

Since the system is a underactuated mechanical system (two joints but only one action), We propose an output function  $y(t) \in R$  as a filtered tracking error given by

$$y(t) = k_1 e_1 + k_2 e_2 + \dot{e}_1 + \dot{e}_2 \tag{17}$$

Where  $k_1$ ,  $k_2$  is a positive constant chosen such that the matrix H of the error system is Huwizt.

According to [27], the method of choosing  $k_1$ ,  $k_2$  so that the following conditions are satisfied, the system will ensure the stability of the uniformly ultimately bounded (UUB).

$$\begin{cases}
P_3 > P_4 \\
0 < k_1 < \frac{P_5}{P_7} \\
k_2 > \frac{k_1 P_4 + P_7}{P_3} + \frac{k_1 P_5 (P_3 - P_4)}{P_3 (P_5 - k_1 P_7)}
\end{cases}$$
(18)

Taking the derivative of Eq.18, we obtain,

$$\dot{y}(t) = k_1 \dot{e}_1 + k_2 \dot{e}_2 + \ddot{e}_1 + \ddot{e}_2 
= k_1 \dot{e}_1 + k_2 \dot{e}_2 + \ddot{q}_{d1} - f_1 - g_1 u - f_2 - g_2 u 
= k_1 \dot{e}_1 + k_2 \dot{e}_2 + \ddot{q}_{d1} - (f_1 + f_2) - (g_1 + g_2) u 
= k_1 \dot{e}_1 + k_2 \dot{e}_2 + \ddot{q}_{d1} - F - G u$$
(19)

Where,  $F = f_1 + f_2$ ,  $G = g_1 + g_2$ 

Remark 1. According to [27], for the case of RIP system, we have

$$g_1 + g_2 < 0, \ \forall |q_2| < arccos(\frac{P_4}{P_2})$$
 (19a)

The inequality (19a) is satisfied for all time  $t \ge 0$ .

**Theorem 1.** Consider the RIP system (1) with the control law given by (20)

$$u = \frac{k_1 \dot{e}_1 + k_2 \dot{e}_2 + \ddot{q}_{d1} - F + \ddot{k}_3 y}{G}$$
(20)

Where  $k_3 > 0$ , the tracking error  $e = [e_1, e_2]^T$  satisfies  $\lim_{t \to \infty} e = 0$ .

**Proof**. The Lyapunov function is selected as,

$$V = \frac{1}{2}y^2 \tag{21}$$

Differentiating V can be obtained,

$$\dot{V} = y\dot{y} = y \left( k_1 \dot{e}_1 + k_2 \dot{e}_2 + \ddot{q}_{d1} - F - Gu \right) \tag{22}$$

Substituting (20) into (22), we can obtain,

$$\dot{V} = y \left( k_1 \dot{e}_1 + k_2 \dot{e}_2 + \ddot{q}_{d1} - F - G \frac{k_1 \dot{e}_1 + k_2 \dot{e}_2 + \ddot{q}_{d1} - F + k_3 y}{G} \right) 
= y \left( k_1 \dot{e}_1 + k_2 \dot{e}_2 + \ddot{q}_{d1} - F - k_1 \dot{e}_1 - k_2 \dot{e}_2 - \ddot{q}_{d1} + F - k_3 y \right) 
= -k_3 y^2 \le 0 
\text{The proof is completed.}$$
(23)

## 3 DESIGNED THE ADAPTIVE NEURAL CONTROLLER

In this section, the study focuses on designing a control system for balancing and tracking the trajectory of a RIP system using an adaptive neural control. Specifically, once the pendulum's swing-up phase transitions into a control area that meets the constraint condition  $q_2$  as defined in Eq. (19a), the adaptive neural control mechanism is activated. A summary of the adaptive neural control block diagram is illustrated in Figure 2.

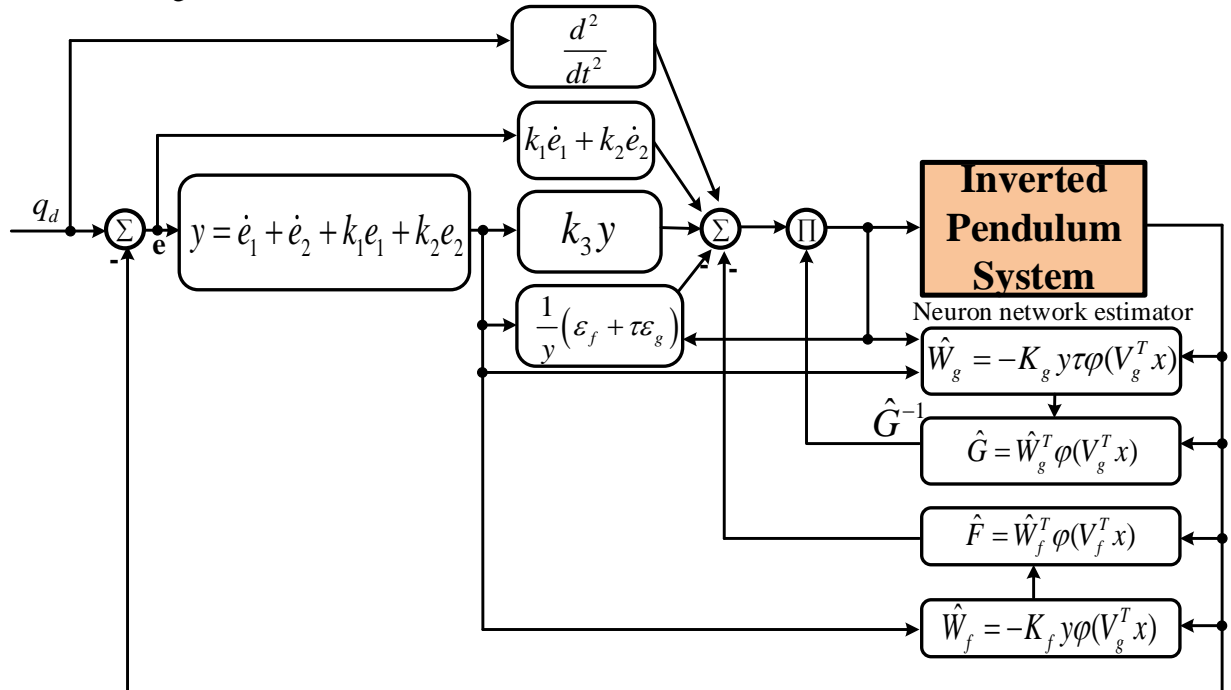


Fig. 2. The block diagram of the proposed controller for RIP system

The details of the components in the block diagram of Figure 2 are designed as follows. When the system parameters are unknown, we do not have a description of F and G. We can approximate F and G functions

through a neural network as follows,

$$F = W_f^T \varphi(V_f^T x) + \varepsilon_f \tag{24}$$

$$G = W_g^T \varphi (V_g^T x) + \varepsilon_g \tag{25}$$

Where,  $\varepsilon_f$ ,  $\varepsilon_g$  are representing the approximate errors of F and G functions. x is an input of neuron x = $[q_1 \ q_2 \ \dot{q_1} \ \dot{q_2} \ 1]^T$ .  $\varphi(.)$  is a hidden layer activation function. The weighting vector  $V = [V_{ij}] \ W =$  $[W_1 \ W_2 \ ... ... W_m]^T$ ,  $i = 1 \div n$ ,  $j = 1 \div m$ . n is the number of neurons of the input layer and m is the number of hidden neurons.

For simplicity, we can choose V as a matrix with randomly selected constant values in a range of [-1; 1]. Therefore, when the system state signals are measured, we design the neural network model to estimate F and G as,

$$\hat{F} = \widehat{W}_f^T \varphi(V_f^T x)$$

$$\hat{G} = \widehat{W}_q^T \varphi(V_q^T x)$$
(26)

$$\widehat{G} = \widehat{W}_g^T \varphi (V_g^T x) \tag{27}$$

The estimated error is defined as,

$$\tilde{F} = F - \hat{F} \approx \tilde{W}_f^T \varphi (V_f^T x) \tag{28}$$

$$\tilde{G} = G - \hat{G} \approx \widetilde{W}_g^T \varphi(V_g^T x) \tag{29}$$

$$\widetilde{W}_f = W_f - \widehat{W}_f; \quad \widetilde{W}_g = W_g - \widehat{W}_g$$
(30)

The proposed neural network-based adaptive control law is given as,

$$u = \frac{k_1 \dot{e}_1 + k_2 \dot{e}_2 + \ddot{q}_{d1} - \hat{F} + k_3 y + u_s}{\hat{G}}$$
(31)

Remark 2. For system (1) and Remark 1, there exist negative boundaries of G function. Without losing generality, we choose the boundary of the function G in the experiment as follows:

$$\begin{cases} \hat{G}(t+1) = -1 \text{ if } |\hat{G}(t)| < -1 \\ \hat{G}(t+1) = \hat{G}(t) \text{ otherwise} \end{cases}$$

**Theorem 2.** Consider the RIP system (1) with the adaptive control law is given by (31),  $\widetilde{W}_f$ ,  $\widetilde{W}_g$  will converge, according to the Barbalat lemma, y(t) will go to zero exponentially as t goes to  $\infty$ .

**Proof.** The Lyapunov function is selected as,
$$V = \frac{1}{2}y^2 + \frac{1}{2}Tr(\widetilde{W}_f^T K_f^{-1} \widetilde{W}_f) + \frac{1}{2}Tr(\widetilde{W}_g^T K_g^{-1} \widetilde{W}_g)$$
(32)

Differentiating V can be obtained,

$$\dot{V} = y\dot{y} + Tr\left(\widetilde{W}_f^T K_f^{-1} \dot{\widetilde{W}}_f\right) + Tr\left(\widetilde{W}_q^T K_q^{-1} \dot{\widetilde{W}}_q\right)$$
(33)

Substituting (19) into (33), we can obtain,

$$\dot{V} = y[k_{1}\dot{e}_{1} + k_{2}\dot{e}_{2} + \ddot{q}_{d1} - F - Gu] + Tr(\widetilde{W}_{f}^{T}K_{f}^{-1}\dot{\widetilde{W}}_{f}) + Tr(\widetilde{W}_{g}^{T}K_{g}^{-1}\dot{\widetilde{W}}_{g})$$

$$= y[k_{1}\dot{e}_{1} + k_{2}\dot{e}_{2} + \ddot{q}_{d1} - F - (\widehat{G} + \widetilde{G})u]$$

$$+ Tr(\widetilde{W}_{f}^{T}K_{f}^{-1}\dot{\widetilde{W}}_{f}) + Tr(\widetilde{W}_{g}^{T}K_{g}^{-1}\dot{\widetilde{W}}_{g}) \tag{34}$$

Substituting (31) into (34), we can obtain,

Substituting (31) into (34), we can obtain,
$$\dot{V} = y \left[ k_1 \dot{e}_1 + k_2 \dot{e}_2 + \ddot{q}_{d1} - F - \hat{G} \left( \frac{k_1 \dot{e}_1 + k_2 \dot{e}_2 + \ddot{q}_{d1} - \hat{F} + k_3 y + u_s}{\hat{G}} \right) - \tilde{G} u \right] \\
+ Tr \left( \widetilde{W}_f^T K_f^{-1} \dot{\widetilde{W}}_f \right) + Tr \left( \widetilde{W}_g^T K_g^{-1} \dot{\widetilde{W}}_g \right) \tag{35}$$

Simplify (35), we get

$$\dot{V} = y(\hat{F} - F - \tilde{G}u - k_3y - u_s) + Tr(\tilde{W}_f^T K_f^{-1} \dot{\tilde{W}}_f) + Tr(\tilde{W}_g^T K_g^{-1} \dot{\tilde{W}}_g) 
= -k_3 y^2 - y\tilde{F} - y\tilde{G}u - Tr(\tilde{W}_f^T K_f^{-1} \dot{\tilde{W}}_f) - Tr(\tilde{W}_g^T K_g^{-1} \dot{\tilde{W}}_g) - yu_s$$
(36)

Substituting (28) and (29) into (36), we can obtain,

$$\dot{V} = -k_3 y^2 - y \widetilde{W}_f^T \varphi(V_f^T x) - y \widetilde{W}_g^T \varphi(V_g^T x) u - Tr \left( \widetilde{W}_f^T K_f^{-1} \dot{\widehat{W}}_f \right) 
- Tr \left( \widetilde{W}_g^T K_g^{-1} \dot{\widehat{W}}_g \right) - y u_s - \varepsilon_f - \varepsilon_g u 
= -k_3 y^2 - Tr \left[ \widetilde{W}_f^T \left( y \varphi(V_f^T x) + K_f^{-1} \dot{\widehat{W}}_f \right) \right]$$

$$-Tr\left[\widetilde{W}_{g}^{T}\left(y\tau\varphi\left(V_{f}^{T}x\right)+K_{g}^{-1}\dot{\widehat{W}}_{g}\right)\right]-yu_{s}-\varepsilon_{f}-\varepsilon_{g}u$$
The weights of neuron update rule and the error compensation signal are chosen as,

$$Tr\left[\widetilde{W}_{f}^{T}\left(y\varphi(V_{f}^{T}x)+K_{f}^{-1}\widehat{W}_{f}\right)\right]=0$$
(38)

$$Tr\left[\widetilde{W}_{g}^{T}\left(yu\varphi(V_{f}^{T}x)+K_{g}^{-1}\widehat{W}_{g}\right)\right]=0$$

$$-yu_{s}-\varepsilon_{f}-\varepsilon_{g}u=0$$
(40)
From (38), (39) and (40), we deduce

$$-yu_s - \varepsilon_f - \varepsilon_g u = 0 \tag{40}$$

$$\dot{\widehat{W}}_f = -K_f y \varphi (V_f^T x) \tag{41}$$

$$\dot{\widehat{W}}_{a} = -K_{a} y u \varphi(V_{f}^{T} x) \tag{42}$$

$$\dot{\hat{W}}_g = -K_g y u \varphi(V_f^T x) 
 u_s = -\frac{1}{y} (\varepsilon_f + \varepsilon_g u)$$
(42)

Substituting (38), (39) and (40) into (37), we can obtain, 
$$\dot{V} = -k_3 y^2 \le 0, \forall k_3 > 0$$
 (44)

The proof is completed.

## RESULTS AND DISCUSSION

#### 4.1 **Simulation results**

The simulation of RIP system has been conducted on MATLAB/Simulink with the following initial conditions. The dynamic parameters (P1, P2, P3, P4, P5, P6, P7) of RIP model [28] are (0.0619, 0.0149, 0.0185, 0.0131, 0.5076, 0.0083, 0.0007), respectively. The control parameters are chosen as  $k_1 = 1, k_2 = 5$ ,  $k_3 = 18$ . Neural networks for estimating function F are chosen as  $K_f = -10$ ,  $k_w = 0.1$ , the number of hidden layer neurons of 10, the matrix V<sub>f</sub> is randomly generated in the range [-1;1], and the activation function is tansig. Neural Networks for estimating function G are chosen as  $K_g = -2.5$ ,  $k_w = 0.35$ , the number of hidden layer neurons is 10, the matrix  $V_g$  is randomly generated in the range [-1;1], and the activation function is logsig. The simulink program of the proposed control for RIP system is described in Fig.3.

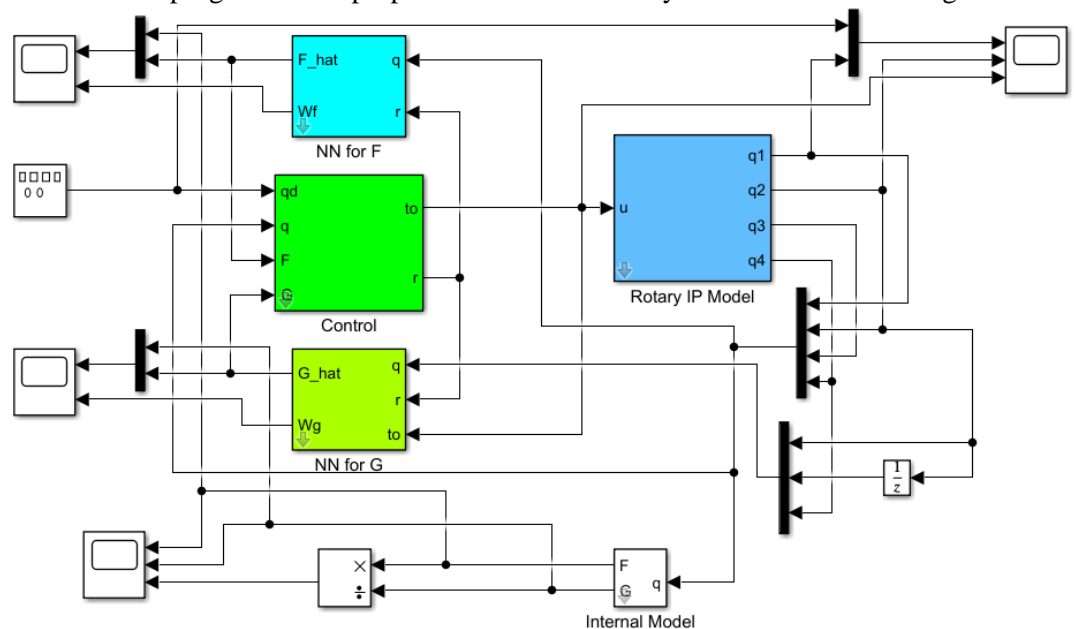


Fig.3. Simulation diagram of the proposed adaptive controller

**Remark 3.** The parameters  $k_1$ ,  $k_2$  were determined through trial and error. While the control laws (20) and (31) are derived using Lyapunov's method, ensuring system stability, these parameters may not represent the optimal control laws for all other underactuated systems.

To verify the performance of the proposed controller, the trajectory references are used including case 1 - sinusoidal signal and case 2 - sinusoidal signal with external disturbance. The results of case 1 are shown in Fig.4, Fig.5, and Fig.6. Fig.4 gives the trajectory tracking of  $q_1$  (link 1 of RIP system),  $q_2$  (link 2 of RIP system), and the control input. We can see that link 1 of RIP system can track the desired sinusoidal signal in 1.6 (sec) and the pendulum (link 2 of RIP system) is close to the upright position (nearly zero).

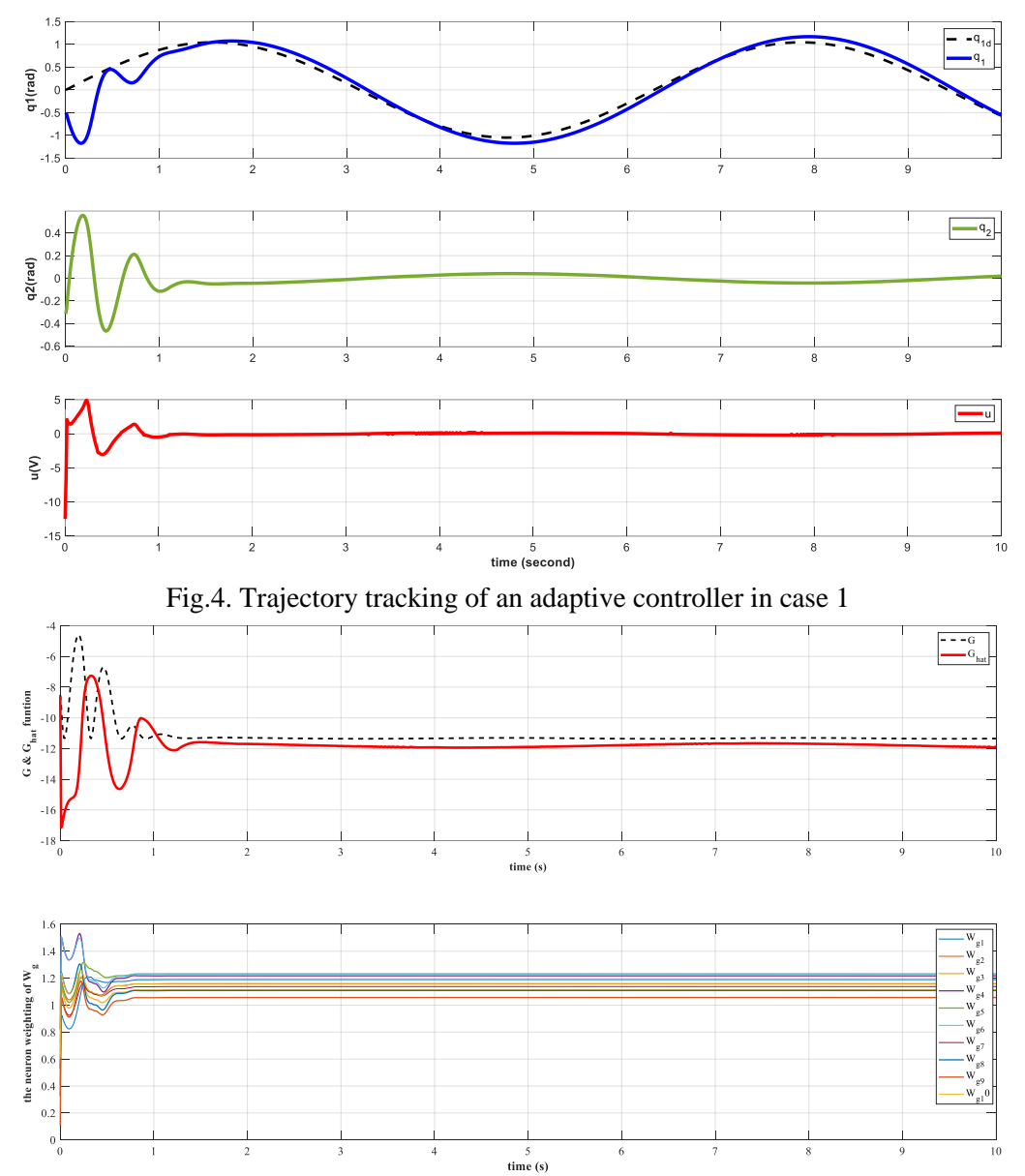


Fig.5. The The estimated results of G function and the convergence of the weights neuron

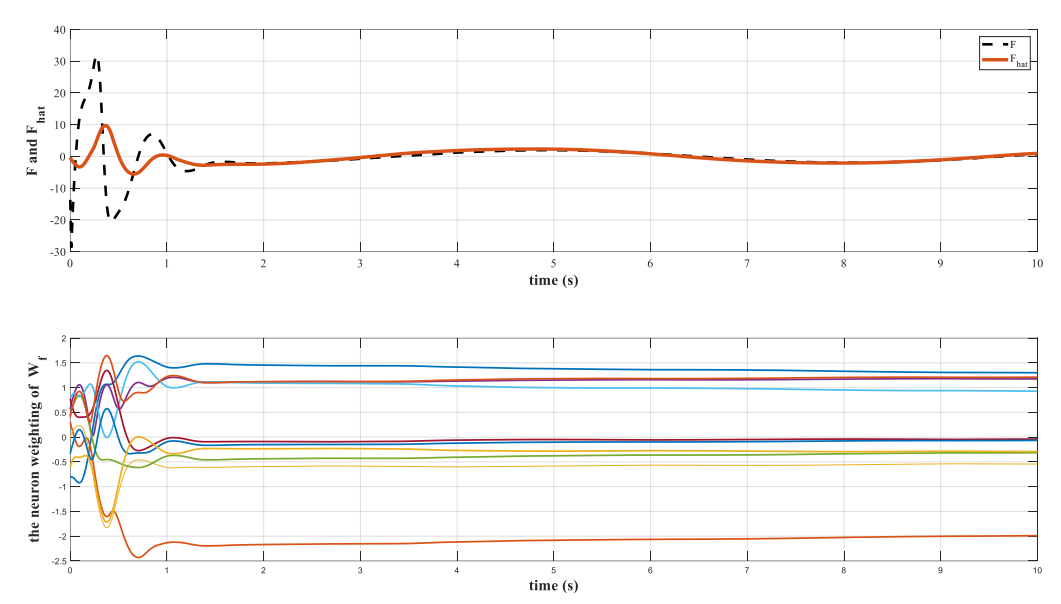


Fig.6. The estimated results of the F function and the convergence of the weights neuron

Fig.5 and Fig.6 show the estimated functions of F and G, and the convergence of the neuron weighting, respectively We can see that the weighs  $W_f$  and  $W_g$  of neural networks will stable after 0.7 (sec) and 3.2 (sec), respectively. This shows the strong adaptability of the proposed controller.

To check the robustness of the controller, an external disturbance as a torque is applied to the pendulum for 0.5 (sec) (case 2) with measurement noise, and the controller performance is evaluated. The other variables with time are displayed in Fig.7.

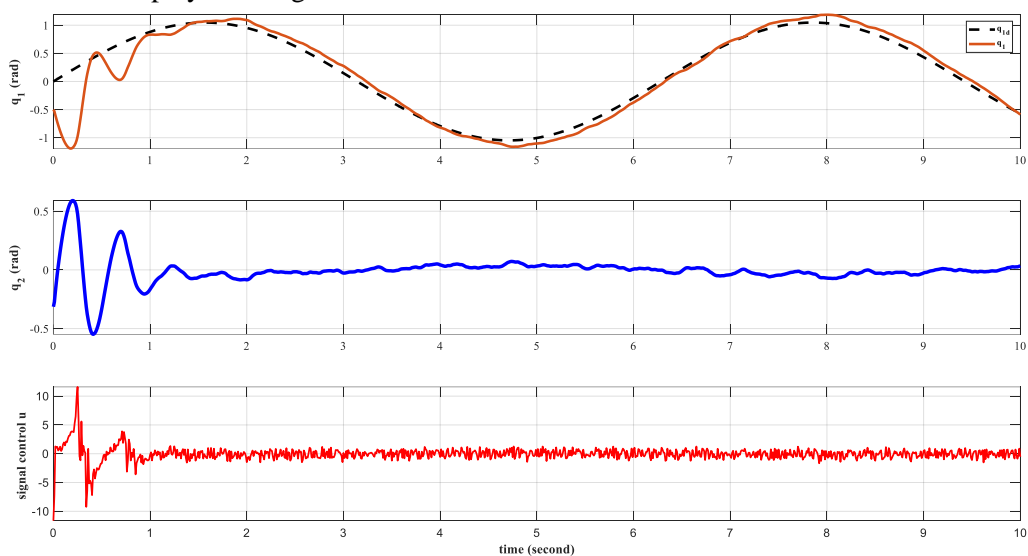


Fig.7. Trajectory tracking of an adaptive controller in case 2

Fig.7 gives the trajectory tracking of  $q_1(\text{link 1 of RIP system})$ ,  $q_2(\text{link 2 of RIP system})$ , and the control input. We can see that the system response is stable, and the output follows the input desired signal well, the network weights converge after 2 seconds. Although RIP parameters change or the noise affects the system, the output response also achieves the desired result.

## 4.2 Experimental results

The experimental RIP system is configured in Fig.8. The diagram of data acquisition and control RIP system with Matlab/Simulink is programmed in Fig.9 and Fig.10. In which, PC is installed Matlab 2013b to implement control with Real-Time Windows Target. National Instrument PCI 6221 board (DAQ) is used to measure the angular of link 1 and link 2 of the RIP system and control the motor DC through the amplifier drive board. Minertia 27V/70W 2000RPM DC motor with encoder 240 pulses/rev is used. The angular

error and angular velocity when sampling at 100Hz  $\pm 0.00654$  rad và  $\pm 0.654$  rad/s, respectively. Motor amplifier drive control with load-bearing parameters is 300W (24V, 15A). Two Encoders 1000 pulses/rev are used to collect the angular link1 and link2 of RIP system. The control parameters are selected as folows,  $k_1 = 2$ ,  $k_2 = 25$ ,  $k_3 = 75$ ,  $K_f = -0.85$ , Kg = -0.65,  $k_{wf} = 0.45$ ,  $k_{wg} = 0.5$ . The number of hidden layers for neural networks is 10.

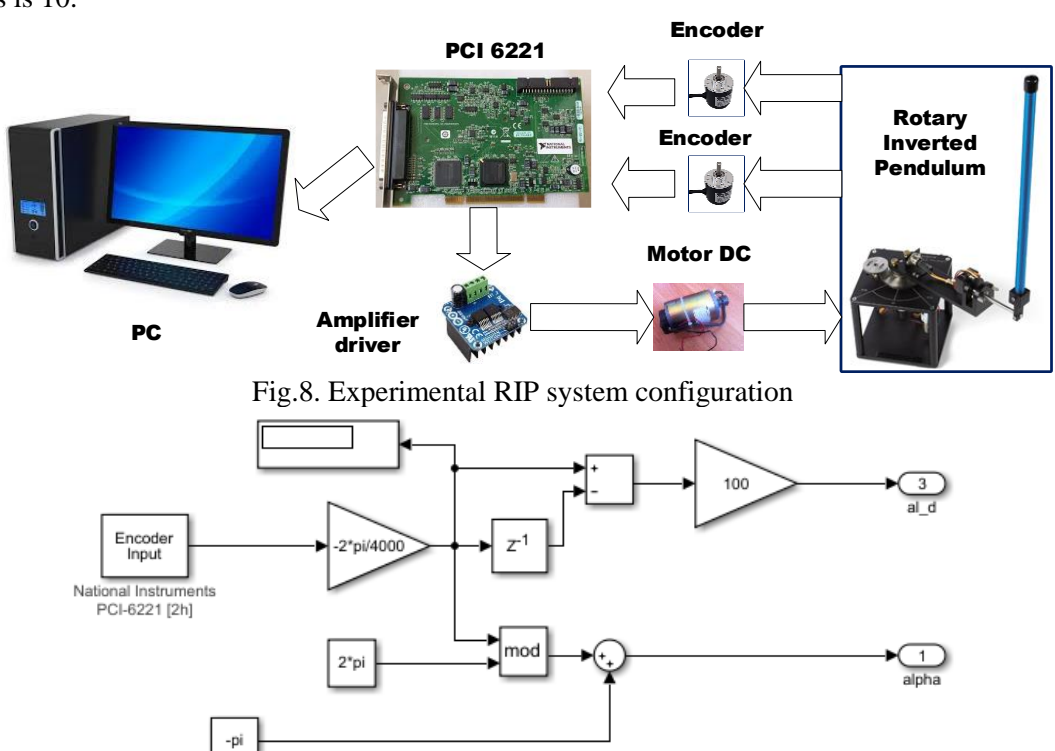


Fig.9. Diagram of data acquisition of RIP through two encoders with Matlab/Simulink

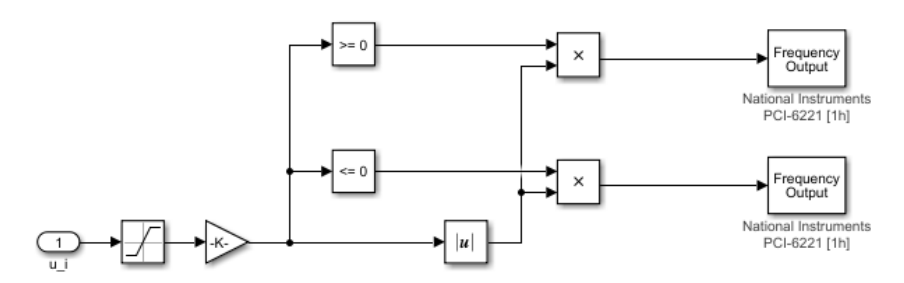


Fig. 10. Diagram of control RIP system with Matlab/Simulink

Case 1. Control RIP system stable at the equilibrium point with external disturbance. Fig.11 to Fig.14 show the trajectory tracking of  $q_1(\text{link 1 of RIP system})$ ,  $q_2(\text{link 2 of RIP system})$ , the control input, and the convergence of the neuron weighting.

Encoder Input tional Instrume PCI-6221 [2h]

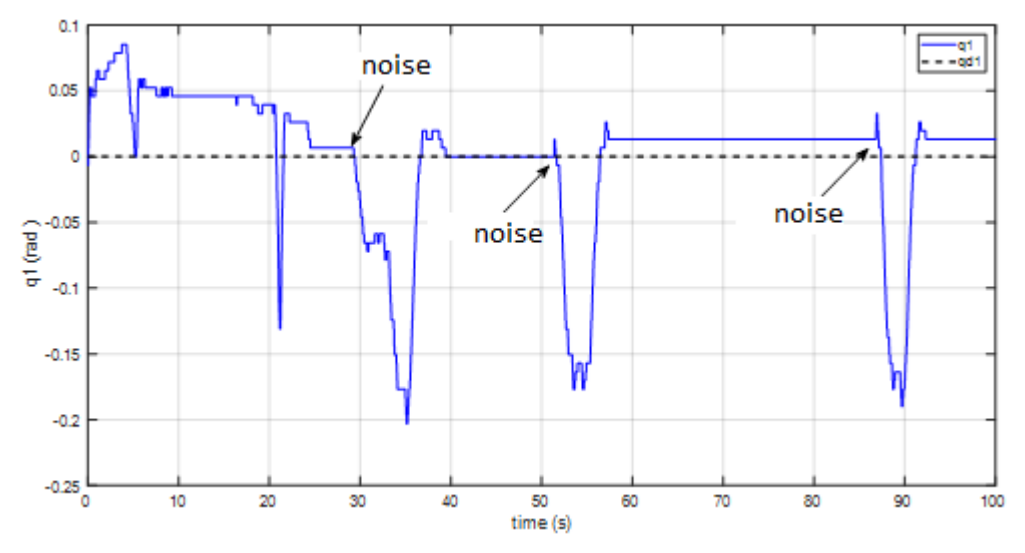
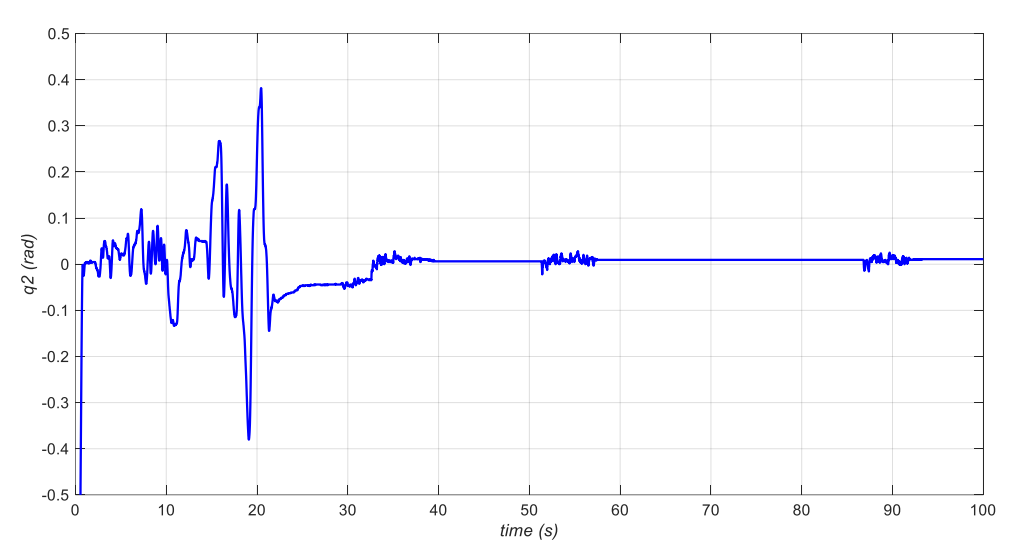


Fig.11. Stable link 1 response results at equilibrium with disturbance



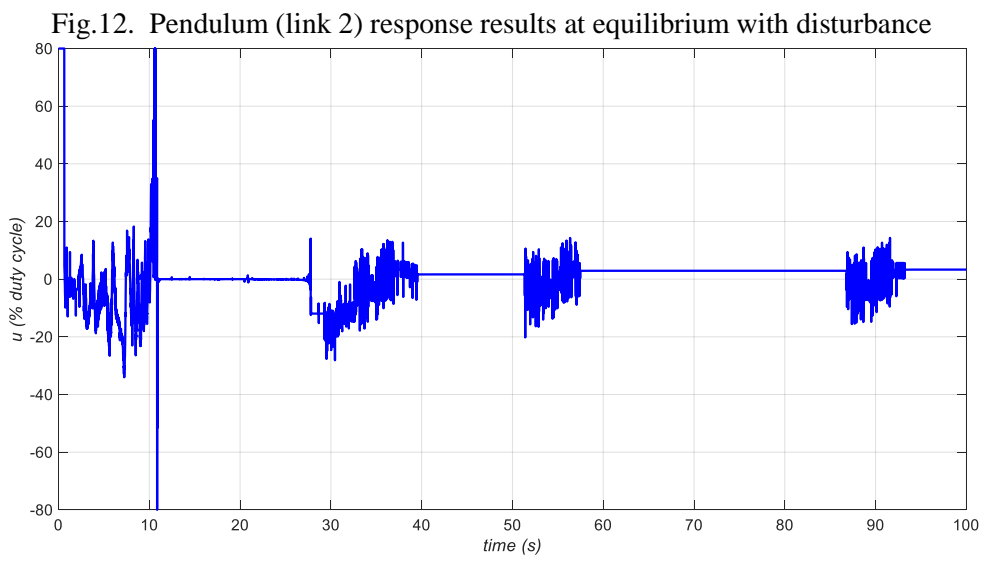


Fig.13. The system control signal is stable at the equilibrium point with disturbance

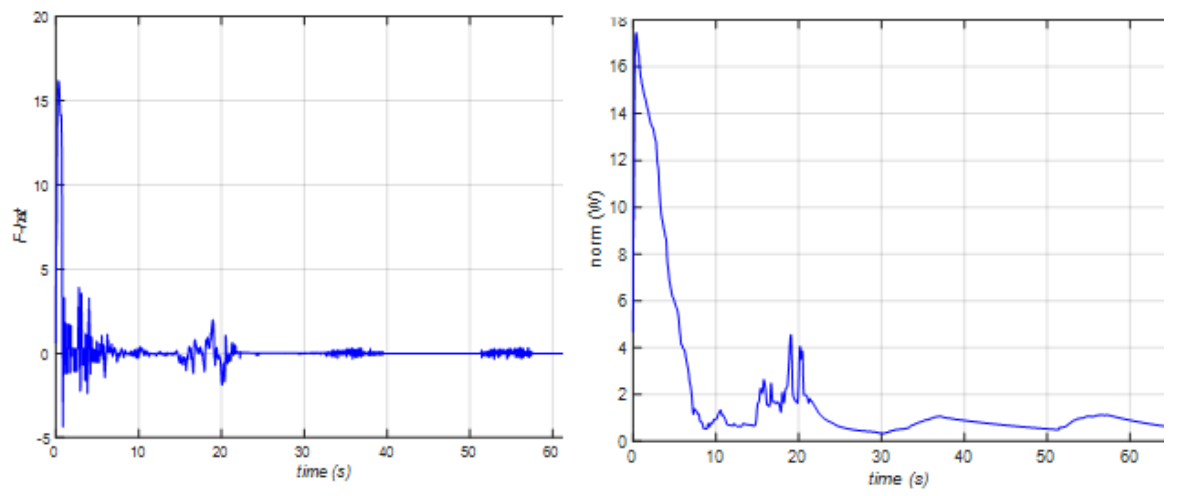


Fig.14. Estimated F(q) and norm weights of neural networks

With the designed network structure and adjusted learning coefficient, as shown in Fig.11 to Fig.14 in the first 20 (sec), the estimated neuron sets have not been the correct value of the system. Then, the values are approximated and the network output and carrier weights gradually update to a value for a stable system in about 8 (sec). At the times of 28 (sec), 52 (sec), 87 (sec), the system output was affected by external noise, the neural network responded well to the role and adjusted the control signal to respond to this change and make for a stable system.

Case 2. Sinusoidal trajectory references with  $\omega = 0.5$  rad/s. Fig.15 to Fig.18 show the trajectory tracking of  $q_1(\text{link 1 of RIP system})$ ,  $q_2(\text{link 2 of RIP system})$ , the control input, and the approximated values of the estimated neuron networks in this case

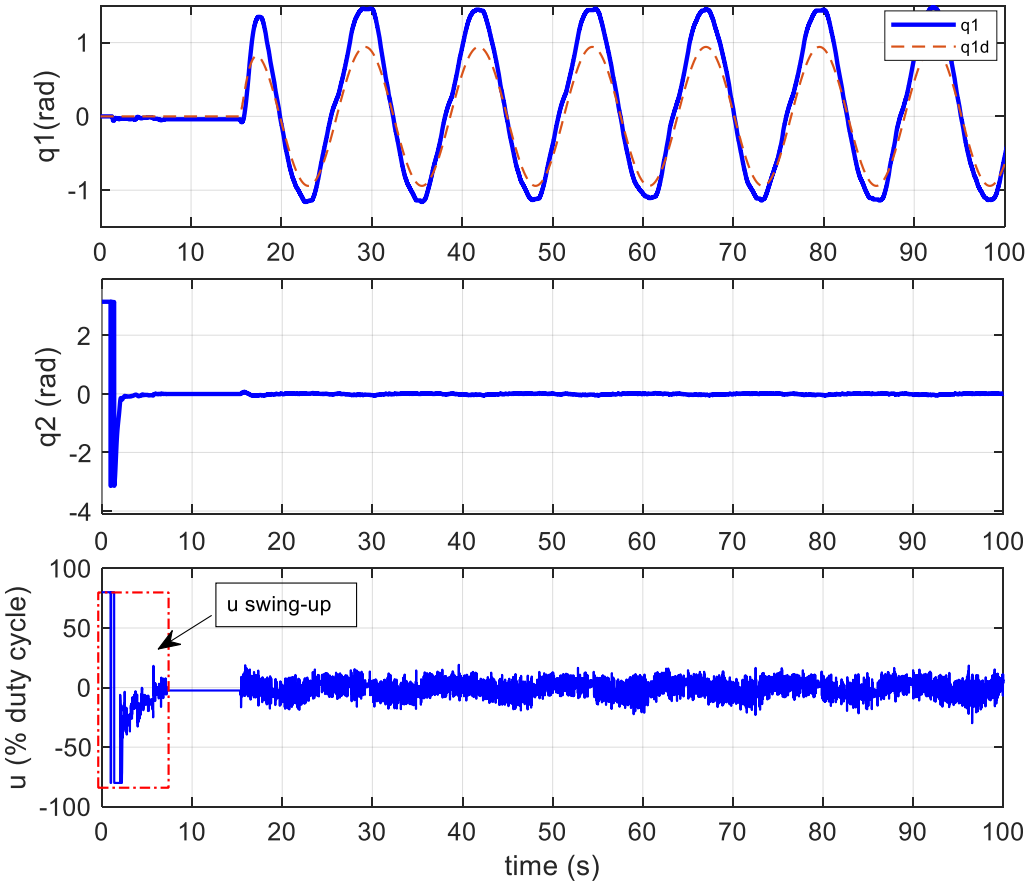


Fig.15. Result of experimental response of manipulator (link 1), pendulum (link 2) and control signal in case 2

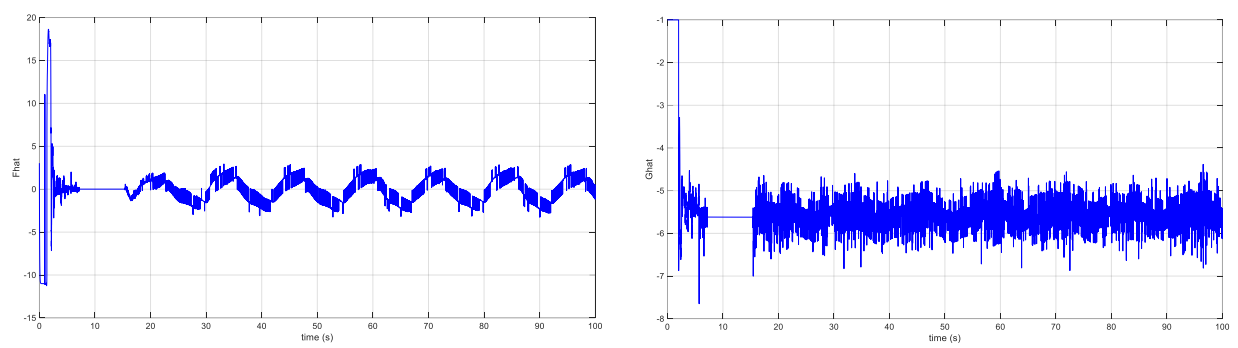


Fig.16. Adaptive approximation of F and G functions in case 2

As can be seen in Figs 15, 16, note that in the first 8 seconds, the system is operating in swing-up mode, moving the pendulum from the stable equilibrium position q2 at pi to the unstable equilibrium position q2 in the domain that satisfies the condition (19a). At about 15 seconds, we control the manipulator (arm) to follow the sine signal with a frequency of 0.5rad/s, the response of the system to follow the desired signal is quite good, although the experimental mechanical system is not of good quality due to being hand-made. The robot arm has tracked the desired sinusoidal signal and the pendulum is well balanced. The estimated values of the G and F functions ensure that the robot follows the set signal and the pendulum remains stable at the above equilibrium position.

Case 3. Sinusoidal trajectory references with  $\omega$  =1.5 rad/s. Fig.17 shows the trajectory tracking of  $q_1(\text{link 1 of RIP system})$ ,  $q_2(\text{link 2 of RIP system})$ , the control input, and the approximated values of the estimated neuron networks

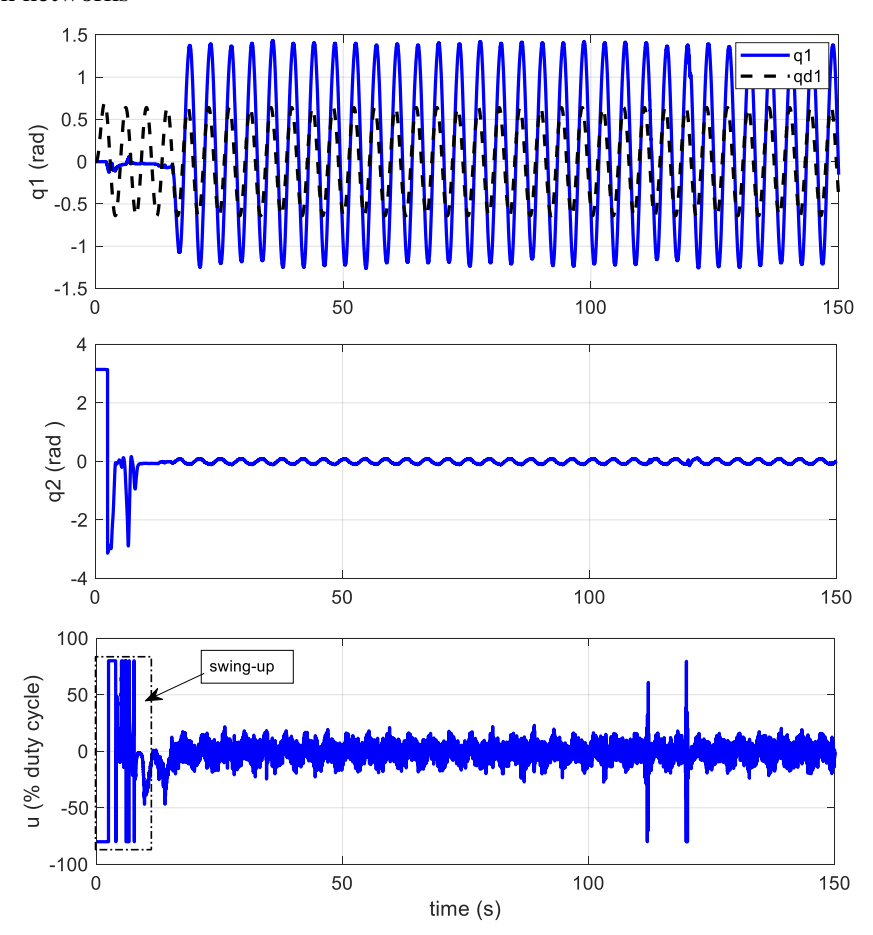
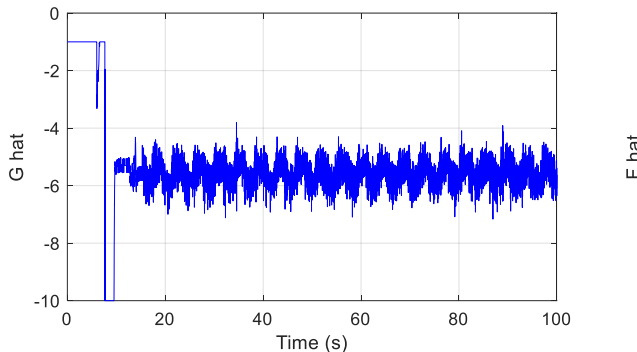


Fig.17. Result of the experimental response of manipulator (link 1), pendulum (link 2) and control signal in case 3



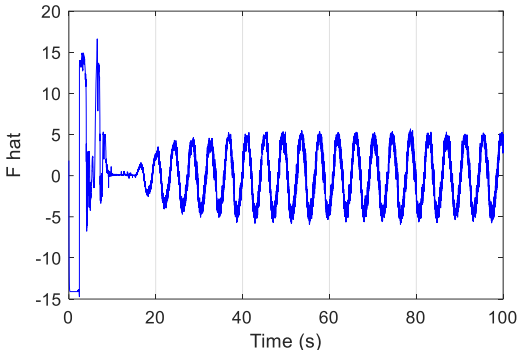


Fig.18. Adaptive approximation of F and G functions in case 3

As can be seen in Figures 17, 18, note that during the first 10 seconds, the system operates in swing-up mode, moving the pendulum from the stable equilibrium position q2 to the unstable equilibrium position q2 in the region satisfying the condition (19a). After the successful Swing up, the adaptive neural control has been tracking the sinusoidal signal with a frequency of 1.5rad/s. The results show that the pendulum remains stable, tracking the reference signal but with a large error.

In summary, the neural adaptive control achieves robustness, balanced control, and good tracking with a sinusoidal reference signal with a frequency change of less than 0.5 rad/2 in the presence of system uncertainty and external disturbances. Despite its potential, the proposed control method still faces limitations, including that we have not specified constraints for the change of the input signal. When the input signal changes with a large amplitude suddenly, the control signal (31) is not updated correctly, leading to system instability. In the control signal (31), there exists a control component  $u_s$  (43) that must ensure the upper and lower bounds for the estimation error of the neural network. If this component is not properly guaranteed, the system will easily become unstable.

## 5 CONCLUSION

This paper showed the development of an adaptive neural network control scheme to control the rotary inverted pendulum (RIP) system with the manipulator (link 1) following the desired input signal and the pendulum (link 2) stabilizes at the equilibrium position. The controller was derived from the universal approximation property of neural networks, and weight adaptation laws were designed. The simulation results clearly indicate the effectiveness of the proposed control law in an uncertain nonlinear underactuated system. The controller simultaneously stabilizes the manipulator's orientation and the angular position of the pendulum. The controller is able to provide robust, non-fluctuation performance in the presence of parametric uncertainty and external disturbances. The proposed adaptive algorithm has also been applied to the experimental RIP system via the DAQ 6221 NI board with Windows RealTime Target. Experimental results also show that the system response follows the desired signal when the kinematic parameters of the system are unknown and there is measurement noise affecting the system. Despite its potential, the proposed control method still has limitations, including the input signal constraints, and upper and lower bounds of the neural network estimation error, which may affect the control quality. These issues will be addressed in future works.

## **REFERENCES**

- [1] M. W. Spong, "Underactuated mechanical systems," in *Control problems in robotics and automation*, Springer, 2005, pp. 135–150.
- [2] X. Xin and Y. Liu, Control design and analysis for underactuated robotic systems. Springer, 2014.
- [3] F. Waheed, I. Khan, and M. Valášek, "A TV-MPC Methodology for Uncertain Under-Actuated Systems: A Rotary Inverted Pendulum Case Study," *IEEE Access*, 2023.
- [4] P. Liu, M. N. Huda, L. Sun, and H. Yu, "A survey on underactuated robotic systems: bio-inspiration, trajectory planning and control," *Mechatronics*, vol. 72, p. 102443, 2020.
- [5] E. Restrepo, A. Loría, I. Sarras, and J. Marzat, "Robust consensus of high-order systems under output constraints: Application to rendezvous of underactuated UAVs," *IEEE Transactions on Automatic Control*, vol. 68, no. 1, pp. 329–342, 2022.

- [6] K. Rsetam, Z. Cao, and Z. Man, "Cascaded-extended-state-observer-based sliding-mode control for underactuated flexible joint robot," *IEEE Transactions on Industrial Electronics*, vol. 67, no. 12, pp. 10822–10832, 2019.
- [7] H. Chen, B. Wang, Z. Hong, C. Shen, P. M. Wensing, and W. Zhang, "Underactuated motion planning and control for jumping with wheeled-bipedal robots," *IEEE Robotics and Automation Letters*, vol. 6, no. 2, pp. 747–754, 2020.
- [8] S. An, X. Wang, L. Wang, and Y. He, "Observer based fixed-time integral sliding mode tracking control for underactuated AUVs via an event-triggered mechanism," *Ocean Engineering*, vol. 284, p. 115158, 2023.
- [9] S.-E. Oltean, "Swing-up and stabilization of the rotational inverted pendulum using PD and fuzzy-PD controllers," *Procedia Technology*, vol. 12, pp. 57–64, 2014.
- [10] Y. Yang, H. H. Zhang, and R. M. Voyles, "Optimal fractional-order proportional-integral-derivative control enabling full actuation of decomposed rotary inverted pendulum system," *Transactions of the Institute of Measurement and Control*, vol. 45, no. 10, pp. 1986–1998, 2023.
- [11] N. J. Mathew, K. K. Rao, and N. Sivakumaran, "Swing up and stabilization control of a rotary inverted pendulum," *IFAC Proceedings Volumes*, vol. 46, no. 32, pp. 654–659, 2013.
- [12] N. P. Nguyen, H. Oh, Y. Kim, and J. Moon, "A nonlinear hybrid controller for swinging-up and stabilizing the rotary inverted pendulum," *Nonlinear Dynamics*, vol. 104, pp. 1117–1137, 2021.
- [13] Z. Ben Hazem, M. J. Fotuhi, and Z. Bingül, "Development of a Fuzzy-LQR and Fuzzy-LQG stability control for a double link rotary inverted pendulum," *Journal of the Franklin Institute*, vol. 357, no. 15, pp. 10529–10556, 2020.
- [14] B. Bekkar and K. Ferkous, "Design of Online Fuzzy Tuning LQR Controller Applied to Rotary Single Inverted Pendulum: Experimental Validation," *Arabian Journal for Science and Engineering*, vol. 48, no. 5, pp. 6957–6972, 2023.
- [15] N. N. Son, C. Van Kien, and H. P. H. Anh, "Uncertain nonlinear system control using hybrid fuzzy LQR-sliding mode technique optimized with evolutionary algorithm," *Engineering Computations*, 2019, doi: 10.1108/ec-08-2018-0356.
- [16] A. Nagarajan and A. A. Victoire, "Optimization Reinforced PID-Sliding Mode Controller for Rotary Inverted Pendulum," *IEEE Access*, vol. 11, pp. 24420–24430, 2023.
- [17] I. Chawla and A. Singla, "Real-time stabilization control of a rotary inverted pendulum using LQR-based sliding mode controller," *Arabian Journal for Science and Engineering*, vol. 46, pp. 2589–2596, 2021.
- [18] X. Yang and X. Zheng, "Swing-up and stabilization control design for an underactuated rotary inverted pendulum system: Theory and experiments," *IEEE Transactions on Industrial Electronics*, vol. 65, no. 9, pp. 7229–7238, 2018.
- [19] R. S. Bhourji, S. Mozaffari, and S. Alirezaee, "Reinforcement Learning DDPG–PPO Agent-Based Control System for Rotary Inverted Pendulum," *Arabian Journal for Science and Engineering*, pp. 1–14, 2023.
- [20] P. N. Dao and Y.-C. Liu, "Adaptive reinforcement learning strategy with sliding mode control for unknown and disturbed wheeled inverted pendulum," *International Journal of Control, Automation and Systems*, vol. 19, no. 2, pp. 1139–1150, 2021.
- [21] F. F. M. El-Sousy, K. A. Alattas, O. Mofid, S. Mobayen, and A. Fekih, "Robust adaptive super-twisting sliding mode stability control of underactuated rotational inverted pendulum with experimental validation," *IEEE Access*, vol. 10, pp. 100857–100866, 2022.
- [22] A. de Carvalho Junior, B. A. Angelico, J. F. Justo, A. M. de Oliveira, and J. I. da Silva Filho, "Model reference control by recurrent neural network built with paraconsistent neurons for trajectory tracking of a rotary inverted pendulum," *Applied Soft Computing*, vol. 133, p. 109927, 2023.
- [23] H. V. Nghi, D. P. Nhien, and D. X. Ba, "A lqr neural network control approach for fast stabilizing rotary inverted pendulums," *International Journal of Precision Engineering and Manufacturing*, vol. 23, pp. 45–56, 2022.
- [24] O. Saleem and K. Mahmood-Ul-Hasan, "Indirect adaptive state-feedback control of rotary inverted pendulum using self-mutating hyperbolic-functions for online cost variation," *IEEE Access*, vol. 8, pp. 91236–91247, 2020.

### ROBUST ADAPTIVE NEURAL TRACKING CONTROL FOR UNDERACTUATED NONLINEAR SYSTEMS...

- [25] Z. Ben Hazem and Z. Bingül, "A comparative study of anti-swing radial basis neural-fuzzy LQR controller for multi-degree-of-freedom rotary pendulum systems," *Neural Computing and Applications*, pp. 1–17, 2023.
- [26] S. Zeghlache, M. Z. Ghellab, A. Djerioui, B. Bouderah, and M. F. Benkhoris, "Adaptive fuzzy fast terminal sliding mode control for inverted pendulum-cart system with actuator faults," *Mathematics and Computers in Simulation*, vol. 210, pp. 207–234, 2023.
- [27] C. Aguilar-Avelar and J. Moreno-Valenzuela, "New feedback linearization-based control for arm trajectory tracking of the furuta pendulum," *IEEE/ASME Transactions on Mechatronics*, vol. 21, no. 2, pp. 638–648, 2015.
- [28] J. Moreno-Valenzuela and C. Aguilar-Avelar, *Motion control of underactuated mechanical systems*, vol. 1. Springer, 2018.

# ĐIỀU KHIỂN NƠ-RON THÍCH NGHI BỀN VỮNG CHO HỆ PHI TUYẾN DƯỚI BÂC: NGHIÊN CỨU TRƯỜNG HỢP CON LẮC NGƯỢC QUAY

NGUYỄN HOÀNG HIẾU, MAI THĂNG LONG, NGUYỄN NGỌC SƠN\*

<sup>1</sup>Khoa Công nghệ Điện tử, trường Đại học Công nghiệp Thành Phố Hồ Chí Minh,

\* Tác giả liên hệ: nguyenngocson@iuh.edu.vn

**Tóm tắt.** Hệ thống bị thiếu điều khiển thể hiện sự tương tác mạnh mẽ và động lực phi tuyến cao, gây ra thách thức cho việc điều khiển chính xác. Bài báo này giới thiệu phương pháp điều khiển thích nghi cho hệ thống con lắc đảo chiều quay (RIP) bị thiếu điều khiển. Mục tiêu là cho cánh tay cơ khí theo dõi quỹ đạo mong muốn và đồng thời duy trì con lắc ở vị trí thẳng đứng. Phương pháp đề xuất sử dụng hai mạng nơron: mạng thứ nhất tập trung vào việc theo dõi quỹ đạo mong muốn của cánh tay cơ khí, trong khi mạng thứ hai ổn định con lắc ở vị trí thẳng đứng. Ôn định hệ thống bằng lý thuyết Lyapunov. Để xác thực hiệu quả của chiến lược điều khiển đề xuất, các thí nghiệm được thực hiện sử dụng thẻ thu thập dữ liệu NI-PCI 6221 với hệ thống RIP. Cả kết quả mô phỏng và thực nghiệm đều nhấn mạnh tính mạnh mẽ của phương pháp điều khiển đề xuất trước các bất định của hệ thống và nhiễu bên ngoài, đạt được hiệu năng vận hành ổn đinh.

Received on February 21 - 2025 Revised on May 25 - 2025